Structural analysis of electrical circuits including magnetoquasistatic devices

Andreas Bartel [a,*], Sascha Baumanns [b], Sebastian Schöps [a]

[a] *Bergische Universität Wuppertal, Lehrstuhl für Angewandte Mathematik und Numerische Mathematik, Gaußstr. 20, 42119 Wuppertal, Germany*
[b] *Universität zu Köln, Mathematisches Institut, Weyertal 86-90, 50931 Köln, Germany*

ARTICLE INFO

ABSTRACT

Modeling electric circuits that contain magnetoquasistatic (MQS) devices leads to a coupled system of differential-algebraic equations (DAEs). In our case, the MQS device is described by the eddy current problem being already discretized in space (via edge-elements). This yields a DAE with a properly stated leading term, which has to be solved in the time domain. We are interested in structural properties of this system, which are important for numerical integration. Applying a standard projection technique, we are able to deduce topological conditions such that the tractability index of the coupled problem does not exceed two. Although index-2, we can conclude that the numerical difficulties for this problem are not severe due to a linear dependency on index-2 variables.

© 2011 IMACS. Published by Elsevier B.V. All rights reserved.

1. Introduction

Usually in a technology computer aided design environment, electric circuits are simulated as networks of basic elements. In this context, devices such as complex semiconductors or even conductors and their interactions are described by corresponding subcircuits. That is, these devices are modeled via equivalent circuits containing only basic elements. Most often, the set-up of equations uses modified nodal analysis (MNA), which we also employ. Today, chip technology develops rapidly and the complexity of the above mentioned devices grows fast and plays a vital role in circuit design. This has two consequences. On the one hand, the corresponding equivalent circuits have become more and more complex and they contain already hundreds of parameters, most of them without a direct physical interpretation, [5]. On the other hand, the device simulation of spatially resolved (complex) models is influenced by secondary effects, such as the surrounding circuitry, which cannot any longer be neglected. This has motivated the idea of using distributed device models, represented by a system of partial differential algebraic equations (PDAEs), to describe the behavior of the devices in the circuit. The resulting mathematical model couples DAEs describing the circuit and PDEs modeling the devices. Thus it gives a set of PDAEs.

To numerically simulate electrical circuits described by such a model, we first discretize the PDEs in space (method of lines). This results in a coupled system of DAE to be solved in simulation.

A DAE is characterized by its index, which roughly measures the equation's sensitivity w.r.t. perturbations of the input and thus it reveals the expected numerical difficulties in simulation. Due to various facts and view points, there are several

---

* Corresponding author.
 E-mail addresses: bartel@math.uni-wuppertal.de (A. Bartel), sbaumann@math.uni-koeln.de (S. Baumanns), schoeps@math.uni-wuppertal.de (S. Schöps).

index definitions, which all generalize the Kronecker index [10]. In this paper, we use as index framework the projector-based tractability index [9,15]. Due to its low smoothness assumptions, this framework is often used in the circuit analysis community. Two further reasons for the tractability index are: (a) it reveals a detailed view on the structure of the equations, (b) for a large class of electric circuits described by equations from MNA, the tractability index is exclusively determined by the circuit's topology (e.g. [7]). Anyhow, considering our network-field system, we expect the same result for other index concepts.

For electric circuits of basic elements refined by distributed elements, there are already a couple of index results. For circuits containing semiconductor devices which are modeled by the drift-diffusion equation, it was shown in [2,18,20,22] that we can extend the topological index criteria of circuits containing just the basic elements.

We investigate electric circuits refined by spatially resolved MQS devices. The structural properties of the corresponding MQS field system, the so-called eddy current problem, was studied first in [23]. There a Kronecker-index analysis is given for the linear 2D problem in the magnetic vector potential formulation. In [18,19], the differential-index was used to obtain more general results for the linear 3D-case, where a gauging becomes necessary to obtain a uniquely solvable formulation. For electric circuits containing MQS devices a topological circuit-condition was shown to be sufficient to yield an overall problem of index-1.

Here, we extend the index analysis of the coupled field/circuit problem to a more general nonlinear setting and to the case of higher index (using the tractability index). The topological conditions for index-1 and index-2 can be shown to be necessary. To this end, we enhance the standard arguments from the tractability index analysis for electric circuits: in the index-1 case we achieve this by adding an additional block of equations and unknowns for the MQS device, and treating both parts as independent as possible. For the index-2 case, we need to follow also an adapted strategy.

This paper is organized as follows. In the next section, we first introduce the models for the electric circuits containing basic network elements and the distributed, but spatially discretized, MQS device models. Then we establish the coupling and state the coupled problem as a DAE. Section 3 contains the main part, which is devoted to the index analysis of the deduced DAE. At the beginning of this section, we roughly recall the basics of the tractability index concept. Then we investigate the structural properties of the electrical circuit including MQS devices. We point out the enhancements needed for transferring the classical index results for electric networks [7] to our coupled system. Eventually, we give a short numerical illustration on the simplest example and finish with conclusions.

2. Modeling

This section contains three parts. First we describe the electric network model including the docking interface for the MQS devices with modeling assumptions. Second we address the space discretized MQS model and related assumptions. Last, the coupled field/circuit system is formulated as coupled DAEs.

2.1. Electric network model

Let us consider an electric network consisting of capacitors, inductors, resistors, voltage and current sources with related incidence matrices (reduced): $\mathbf{A}_C, \mathbf{A}_R, \mathbf{A}_L, \mathbf{A}_V$ and $\mathbf{A}_I$, which state the node–branch relation for each element type for the underlying digraph:

$$\left(\mathbf{A}_\star\right)_{ij} = \begin{cases} 1, & \text{if branch } j \text{ leaves node } i, \\ -1, & \text{if branch } j \text{ enters node } i, \\ 0, & \text{if branch } j \text{ is not incident with node } i. \end{cases}$$

In fact, each row of $\mathbf{A}_\star$ refers to a network node. As usual, one node is identified as mass (or ground) node and the corresponding row is skipped in $\mathbf{A}_\star$.

The MNA leads to equations of the form (see e.g. [7])

$$\mathbf{A}_C \frac{\mathrm{d}}{\mathrm{d}t} \mathbf{q}_C\left(\mathbf{A}_C^\top \mathbf{e}, t\right) + \mathbf{A}_R \mathbf{g}_R\left(\mathbf{A}_R^\top \mathbf{e}, t\right) + \mathbf{A}_L \mathbf{j}_L + \mathbf{A}_V \mathbf{j}_V + \mathbf{A}_I \mathbf{i}_s(t) = 0, \tag{1a}$$

$$\frac{\mathrm{d}}{\mathrm{d}t} \boldsymbol{\Phi}_L\left(\mathbf{j}_L, t\right) - \mathbf{A}_L^\top \mathbf{e} = 0, \tag{1b}$$

$$\mathbf{A}_V^\top \mathbf{e} - \mathbf{v}_s(t) = 0 \tag{1c}$$

with time $t \in \mathcal{I}$, $\mathcal{I} = [t_0, T] \subset \mathbb{R}$. The given vector functions $\mathbf{q}_C(\mathbf{v}, t)$, $\mathbf{g}_R(\mathbf{v}, t)$, $\boldsymbol{\Phi}_L(\mathbf{j}, t)$, $\mathbf{v}_s(t)$ and $\mathbf{i}_s(t)$ describe the constitutive relations for the circuit elements (for charge, resistance, flux, voltage source and current source, respectively). The unknowns are the node potentials $\mathbf{e} : \mathcal{I} \to \mathbb{R}^n$, except of the mass node, as well as the currents $\mathbf{j}_L : \mathcal{I} \to \mathbb{R}^{n_L}$ through inductors and the currents $\mathbf{j}_V : \mathcal{I} \to \mathbb{R}^{n_V}$ through voltage sources (for n_L inductors and n_V voltage sources, respectively). The potential at the mass node is assigned to zero. Thus (1a) states the current balance at each network node, and (1b) and (1c) state the constitutive relations for inductances and voltage sources, respectively. Details can found in e.g. [22,7].

For the later analysis loops and cutsets of branches will play a key role. A subset of branches of a connected graph is a cutset if and only if the deletion of that subset results in a disconnected graph and the deletion of any proper subset of that

subset does not disconnect the graph. The definition of a loop (or circle) is clear. A tree is a subset of branches containing all nodes but no loops. For a mathematically consistent description, we need:

Assumption 2.1 *(Soundness of circuits).* The circuit is connected. It contains neither loops of voltage sources only nor cutsets of current sources only. The topological conditions translate into matrix conditions as:

$$\mathbf{A}_V \quad \text{and} \quad \begin{bmatrix} \mathbf{A}_C \, \mathbf{A}_R \, \mathbf{A}_L \, \mathbf{A}_V \end{bmatrix}^\top \quad \text{have full column rank.}$$

If Assumption 2.1 is violated, the circuit equations (plus initial conditions) would have either no solution or infinite many solutions due to Kirchhoff's laws.

Remark 2.2 *(Incidence matrices).* We note the following (our incidence matrices are always reduced):

(a) An incidence matrix $\mathbf{A}_X$ of a subgraph has full column rank if and only if there is no loop (in the subgraph), i.e., no X-loop.
(b) Let $[\mathbf{A}_X, \mathbf{A}_Y]$ denote the incidence matrix of a connected graph. Then $\mathbf{A}_X^\top$ has full column rank if and only if there is a spanning tree of elements from $\mathbf{A}_Y$.
Moreover for $[\mathbf{A}_X, \mathbf{A}_Y]$ connected, $\mathbf{A}_Y^\top$ has full column rank if and only if the graph contains no cutset of elements from $\mathbf{A}_X$ (no X-cutset).

Assumption 2.3 *(Local passivity).* The functions $\mathbf{q}_C(\mathbf{v}, t)$, $\boldsymbol{\Phi}_L(\mathbf{j}, t)$ and $\mathbf{g}_R(\mathbf{v}, t)$ are continuous differentiable with positive definite Jacobians:

$$\mathbf{C}(\mathbf{v}, t) := \frac{\partial \mathbf{q}_C(\mathbf{v}, t)}{\partial \mathbf{v}}, \qquad \mathbf{L}(\mathbf{j}, t) := \frac{\partial \boldsymbol{\Phi}(\mathbf{j}, t)}{\partial \mathbf{j}}, \qquad \mathbf{G}(\mathbf{v}, t) := \frac{\partial \mathbf{g}_R(\mathbf{v}, t)}{\partial \mathbf{v}}.$$

Next, we add the electromagnetic field-elements to our system. That is, we enlarge our list of basic elements by an field element (precisely an MQS device), which shall consist of a number of n_M separated conductors coupled inductively using field equations. This gives an extended circuit. In the MNA framework, we simply add the unknown current $\mathbf{j}_M \in \mathbb{R}^{n_M}$ through the MQS device to the current balance equation (1a) using the corresponding incidence matrix $\mathbf{A}_M$. Then (1a) reads

$$\mathbf{A}_C \frac{\mathrm{d}}{\mathrm{d}t} \mathbf{q}_C\big(\mathbf{A}_C^\top \mathbf{e}, t\big) + \mathbf{A}_R \mathbf{g}_R\big(\mathbf{A}_R^\top \mathbf{e}, t\big) + \mathbf{A}_L \mathbf{j}_L + \mathbf{A}_V \mathbf{j}_V + \mathbf{A}_I \mathbf{i}_s(t) + \mathbf{A}_M \mathbf{j}_M = 0. \tag{2}$$

To obtain a uniquely solvable system we need further equations for the MQS device which describe the unknown currents $\mathbf{j}_M$ in terms of the other variables. This will involve the applied potentials $\mathbf{A}_M^\top \mathbf{e}$. Before we discuss this, we now restate (2.1) for our extended circuit:

Assumption 2.4 *(Soundness of extended circuit).* The circuit is connected and the matrices

$$\mathbf{A}_V \quad \text{and} \quad [\mathbf{A}_C \, \mathbf{A}_R \, \mathbf{A}_L \, \mathbf{A}_V \, \mathbf{A}_M] \quad \text{have full column rank,}$$

i.e., there is neither a loop containing only voltage sources nor a cutset containing only current sources.

Remark 2.5. In stating the model as we do, we implicitly assume independent voltage and current sources only. Our results can be extended to a broad class of controlled sources [7].

2.2. MQS device models

Next, we derive the MQS device model from Maxwell's space-discrete equations on a staggered grid pair. They can be obtained from any spatial discretization of Maxwell's equations on a bounded domain $\boldsymbol{\Omega}$, here we use the notation of the finite integration technique, [24],

$$\mathbf{C}\widehat{\mathbf{e}} = -\frac{\mathrm{d}}{\mathrm{d}t}\widehat{\widehat{\mathbf{b}}}, \qquad \tilde{\mathbf{C}}\widehat{\mathbf{h}} = \frac{\mathrm{d}}{\mathrm{d}t}\widehat{\widehat{\mathbf{d}}} + \widehat{\widehat{\mathbf{j}}}, \qquad \tilde{\mathbf{S}}\widehat{\widehat{\mathbf{d}}} = \mathbf{q}, \qquad \mathbf{S}\widehat{\widehat{\mathbf{b}}} = 0 \tag{3}$$

with discrete curl operators $\mathbf{C}$ and $\tilde{\mathbf{C}}$, divergence operators $\mathbf{S}$ and $\tilde{\mathbf{S}}$ (on the staggered grids). The variables are line-integrals of electric and magnetic field strength $\widehat{\mathbf{e}}$ and $\widehat{\mathbf{h}}$ (edges of the cells), respectively, and surface integrals of source current density, discrete magnetic flux density and displacement field $\widehat{\widehat{\mathbf{j}}}$, $\widehat{\widehat{\mathbf{b}}}$ and $\widehat{\widehat{\mathbf{d}}}$. Maxwell's equations are closed with the constitutive material relations:

$$\widehat{\mathbf{h}} = \mathbf{M}_\nu \widehat{\widehat{\mathbf{b}}}, \qquad \widehat{\widehat{\mathbf{d}}} = \mathbf{M}_\varepsilon \widehat{\mathbf{e}}, \qquad \widehat{\widehat{\mathbf{j}}} = \mathbf{M}_\sigma \widehat{\mathbf{e}}, \tag{4}$$

where matrices $\mathbf{M}_\nu = \mathbf{M}_\nu(\widehat{\widehat{\mathbf{b}}})$, $\mathbf{M}_\varepsilon$ and $\mathbf{M}_\sigma$ represent the reluctivities (without hysteresis effects), permittivities and conductivities.

For low frequencies ("eddy current problem") the displacement current density can be neglected with respect to the current density (on the whole domain), [11]:

$$\max\left|\frac{\mathrm{d}}{\mathrm{d}t}\widehat{\widehat{\mathbf{d}}}\right| \ll \max|\widehat{\widehat{\mathbf{j}}}|.$$

Furthermore, we can reformulate the problem in terms of the line-integrated magnetic vector potential $\widehat{\mathbf{a}} : \mathcal{I} \to \mathbb{R}^{n_a}$ (where n_a denotes the number of primary edges) and the electric scalar potential $\boldsymbol{\Phi}$

$$\widehat{\mathbf{e}} = -\frac{\mathrm{d}}{\mathrm{d}t}\widehat{\mathbf{a}} + \tilde{\mathbf{S}}^\top\boldsymbol{\Phi} \quad \text{and} \quad \widehat{\widehat{\mathbf{b}}} = \mathbf{C}\widehat{\mathbf{a}}. \tag{5}$$

Starting from Ampère's law (second equation of (3)) neglecting the displacement current density, inserting material relations and using $\widehat{\mathbf{a}}$, this yields the following first-order DAE ("curl–curl equation"):

$$\mathbf{M}\frac{\mathrm{d}}{\mathrm{d}t}\widehat{\mathbf{a}} + \tilde{\mathbf{C}}\mathbf{M}_\nu(\mathbf{C}\widehat{\mathbf{a}})\mathbf{C}\widehat{\mathbf{a}} = \mathbf{M}\tilde{\mathbf{S}}^\top\boldsymbol{\Phi}, \tag{6}$$

with the constant conductivity matrix $\mathbf{M} := \mathbf{M}_\sigma$ and the curl–curl matrix $\tilde{\mathbf{C}}\mathbf{M}_\nu(\mathbf{C}\widehat{\mathbf{a}})\mathbf{C}$, which depends nonlinearly on the magnitude of the flux $\widehat{\widehat{\mathbf{b}}}$ modeling ferromagnetic saturation. During time-integrating of the curl–curl equation, the matrix pencil (evaluated for a given $\widehat{\mathbf{a}}$)

$$\left[\mathbf{M}, \frac{\partial}{\partial\widehat{\mathbf{a}}}\big(\tilde{\mathbf{C}}\mathbf{M}_\nu(\mathbf{C}\widehat{\mathbf{a}})\mathbf{C}\widehat{\mathbf{a}}\big)\right] := \lambda\mathbf{M} + \frac{\partial}{\partial\widehat{\mathbf{a}}}\big(\tilde{\mathbf{C}}\mathbf{M}_\nu(\mathbf{C}\widehat{\mathbf{a}})\mathbf{C}\widehat{\mathbf{a}}\big) \qquad \text{for } \lambda > 0$$

occurs naturally as the system matrix. In the implicit Euler scheme, λ is the reciprocal time step. The pencil is singular because of the constant kernel

$$\operatorname{Ker}\mathbf{M} \cap \operatorname{Ker} \frac{\partial}{\partial\widehat{\mathbf{a}}}\big(\tilde{\mathbf{C}}\mathbf{M}_\nu(\mathbf{C}\widehat{\mathbf{a}})\mathbf{C}\widehat{\mathbf{a}}\big) \neq \{0\} \quad \text{for all } \widehat{\mathbf{a}}.$$

Non-conducting areas and the nontrivial kernel of the curl operator (in 3D) are the algebraic origin and a regularization can remove the common kernel from the matrix pencil [3].

Assumption 2.6 *(Gauge).* We assume a regularization of (6)

$$\mathbf{K}(\widehat{\mathbf{a}}) := \tilde{\mathbf{C}}\mathbf{M}_\nu(\widehat{\mathbf{a}})\mathbf{C} + \mathbf{Y} \quad \text{and} \quad \mathbf{k}'_a(\widehat{\mathbf{a}}) := \frac{\partial}{\partial\widehat{\mathbf{a}}}\big(\tilde{\mathbf{C}}\mathbf{M}_\nu(\widehat{\mathbf{a}})\mathbf{C}\widehat{\mathbf{a}}\big) + \mathbf{Y} \tag{7}$$

with a positive semi-definite matrix $\mathbf{Y}$ such that $\mathbf{K}$ and $\mathbf{k}'_a$ are positive definite for elements in $\ker\mathbf{M}$, e.g. [3].

Assumption 2.6 guarantees that the matrix pencil $[\mathbf{M}, \mathbf{k}'_a]$ is positive definite, i.e., $\widehat{\mathbf{a}}^\top(\alpha\mathbf{M} + \mathbf{k}'_a)\widehat{\mathbf{a}} > 0$ for all $\widehat{\mathbf{a}} \neq \mathbf{0}$ and $\lambda > 0$. Notice that in Assumption 2.6 both matrices $\mathbf{K}$ and $\mathbf{k}'_a$ may still be only positive semi-definite.

As boundary conditions we assume that the tangential component of the vector potential $\widehat{\mathbf{a}}$ vanishes at the boundary of the domain (Dirichlet).

2.2.1. MQS-device and coupling

The coupling of the MQS device to the circuit is established by a conductive subdomain $\boldsymbol{\Omega}_\mathrm{M} \subset \boldsymbol{\Omega}$ which identifies the areas, where an electric current is imposed by the coupled circuit. In this subdomain the electric scalar potential $\boldsymbol{\Phi}$ is related to the circuit voltage drop $\mathbf{v}_\mathrm{M}$ and the integrated current density $\widehat{\widehat{\mathbf{j}}}$ is related to the branch current $\mathbf{j}_\mathrm{M}$ of the electric circuit.

Let us consider a single solid conductor (see Fig. 1) with two perfect conducting contacts. The 0D-voltage drops must be distributed onto the 3D-grid; this defines an applied electric field on the edges. Since we are only interested in the line integrals of this field, let $\gamma \in \{-1, 0, 1\}^{n_a}$ be a path from one contact to the other (within $\boldsymbol{\Omega}_\mathrm{M}$). Due to the linearity of Ohm's law (equation three in (4)), it is sufficient to consider an applied voltage $\mathbf{v}_\mathrm{M} = 1$ V and define a corresponding distribution vector $\tilde{\mathbf{X}} \in \mathbb{R}^{n_a}$, such that $\tilde{\mathbf{X}}^\top\gamma = 1$. A computationally beneficial choice [4] is to impose the voltages only onto the edges crossing a reference plane (see Fig. 1). This yields a sparse distribution vector (here given for the Cartesian case with an aligned, orthogonal reference plane, Fig. 1):

$$(\tilde{\mathbf{X}})_i = \begin{cases} \pm 1 & \text{if edge } i \text{ crosses the reference plane,} \\ 0 & \text{else,} \end{cases}$$

where the sign depends on the directions of the edges. Already this vector defines a valid unit excitation for (6) as:
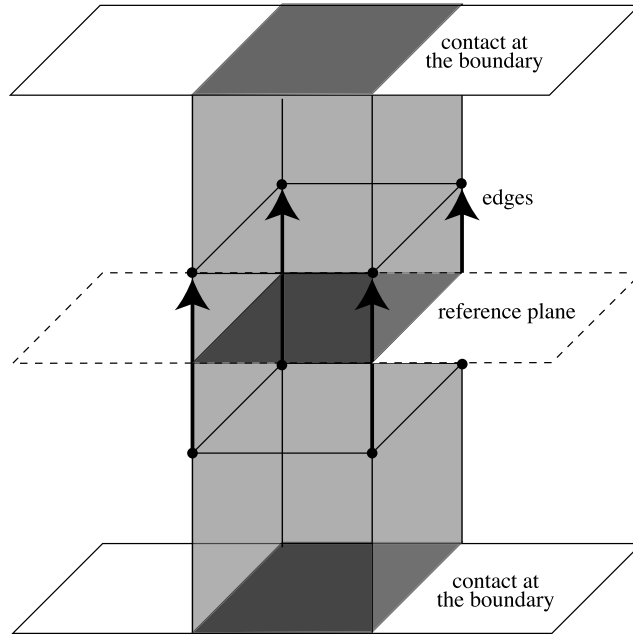
Fig. 1. Coupling as given as in [4] (for a Cartesian grid).

$$\tilde{\mathbf{S}}^\top \boldsymbol{\Phi} := \tilde{\mathbf{X}} \mathbf{v}_M \quad \text{(with } \mathbf{v}_M = 1\text{V)}. \tag{8}$$

The excitation $\mathbf{v}_M$ defines an applied electric field $\tilde{\mathbf{S}}^\top \boldsymbol{\Phi}$, whose integrated current density is not divergence-free: $\tilde{\mathbf{S}} \mathbf{M} \tilde{\mathbf{X}}_M \mathbf{v}_M \neq 0$. Thus we favor the construction of an excitation vector $\mathbf{X}$ yielding a divergence-free current. For this construction, we solve the Poisson problem, [4]

$$\tilde{\mathbf{S}} \mathbf{M} \tilde{\mathbf{S}}^\top \boldsymbol{\Phi}_M = \tilde{\mathbf{S}} \mathbf{M} \tilde{\mathbf{X}} \mathbf{v}_M \tag{9}$$

for the given vector $\tilde{\mathbf{X}}$ and defining the new excitation vector as

$$\mathbf{X} := \tilde{\mathbf{X}} - \tilde{\mathbf{S}}^\top \boldsymbol{\Phi}_M.$$

The distribution vector $\mathbf{X}$ is less sparse than $\tilde{\mathbf{X}}$, but it yields a divergence-free current by construction. Now, we use $\mathbf{X}$ instead of $\tilde{\mathbf{X}}$ in (8) and apply any voltage drop $\mathbf{v}_M$. By linearity, this gives the general excitation

$$\tilde{\mathbf{S}}^\top \boldsymbol{\Phi} := \mathbf{X} \mathbf{v}_M \tag{10}$$

and states the circuit-to-MQS device coupling, where voltages are obtained from the circuit by $\mathbf{v}_M = \mathbf{A}_M^\top \mathbf{e}$. Inserted the exitation (10) into (6) results in

$$\mathbf{M} \frac{\mathrm{d}}{\mathrm{d}t} \widehat{\mathbf{a}} + \mathbf{K}(\widehat{\mathbf{a}}) \widehat{\mathbf{a}} = \mathbf{M} \mathbf{X} \mathbf{v}_M. \tag{11}$$

The total current through the conductor is given by integrating over the cross section. We find by using Ohm's Law

$$\mathbf{j}_M = \mathbf{X}^\top \widehat{\widehat{\mathbf{j}}} = \mathbf{X}^\top \mathbf{M} \widehat{\mathbf{e}} = \mathbf{X}^\top \mathbf{M} \mathbf{X} \mathbf{v}_M - \mathbf{X}^\top \mathbf{M} \frac{\mathrm{d}}{\mathrm{d}t} \widehat{\mathbf{a}}$$

or equivalently (using the curl–curl equation (11))

$$\mathbf{j}_M = \mathbf{X}^\top \mathbf{K}(\widehat{\mathbf{a}}) \widehat{\mathbf{a}}, \tag{12}$$

which states the MQS device-to-circuit coupling.

In the case of a multiport MQS device ($n_M > 1$), e.g., a transformer with two coils, several coupling vectors must be constructed as explained above. Then the coupling is carried out in several (disjunct) subdomains by a coupling matrix $\mathbf{X} \in \mathbb{R}^{n_a \times n_M}$.

Remark 2.7. Special choices of the conductivity matrix $\mathbf{M}$ yield certain conductor models (e.g. stranded or foil conductors). Still, using algebraic manipulations, the coupling can be brought into the structure of (11) and (12), [19].

2.3. Coupled problem

Assembling the equations of the MNA (2), (1b), (1c) for the extended circuit and the space discrete Maxwell equations (11), we can formulate the field/circuit coupled system

$$\mathbf{A}_C\frac{\mathrm{d}}{\mathrm{d}t}\mathbf{q}_C\big(\mathbf{A}_C^\top\mathbf{e},t\big)+\mathbf{A}_R\mathbf{g}_R\big(\mathbf{A}_R^\top\mathbf{e},t\big)+\mathbf{A}_L\mathbf{j}_L+\mathbf{A}_V\mathbf{j}_V+\mathbf{A}_I\mathbf{i}_s(t)+\mathbf{A}_M\mathbf{X}^\top\mathbf{K}_\nu(\widehat{\mathbf{a}})\widehat{\mathbf{a}}=0,$$

$$\frac{\mathrm{d}}{\mathrm{d}t}\boldsymbol{\Phi}_L\big(\mathbf{j}_L,t\big)-\mathbf{A}_L^\top\mathbf{e}=0,$$

$$\mathbf{A}_V^\top\mathbf{e}-\mathbf{v}_s(t)=0,$$

$$\mathbf{M}\frac{\mathrm{d}}{\mathrm{d}t}\widehat{\mathbf{a}}+\mathbf{K}(\widehat{\mathbf{a}})\widehat{\mathbf{a}}-\mathbf{M}\mathbf{X}\mathbf{A}_M^\top\mathbf{e}=0, \tag{13}$$

where the MQS-current (12) is already inserted into the current balance (2). The unknows of (13) are $\mathbf{e}$, $\mathbf{j}_L$, $\mathbf{j}_V$, $\widehat{\mathbf{a}}$. For this system with these unknowns, we will derive the structural analysis in the following.

3. Index analysis

The tractability index is a projector-based approach. It provides an index characterization in terms of the original problem's unknowns, leads to a precise solution description and requires low smoothness of the involved functions [9,15]. First, we summarize the key ingredients, then we apply the index concept to our coupled problem.

3.1. Tractability index

We investigate the DAE

$$\mathbf{A}\frac{\mathrm{d}}{\mathrm{d}t}\mathbf{d}(\mathbf{x},t)+\mathbf{b}(\mathbf{x},t)=0 \tag{14}$$

with constant matrix $\mathbf{A}\in\mathbb{R}^{m\times n}$, coefficient functions $\mathbf{d}(\mathbf{x},t)\in\mathbb{R}^n$ and $\mathbf{b}(\mathbf{x},t)\in\mathbb{R}^m$. We assume both coefficient functions to be continuous and that continuous partial derivatives $\mathbf{d}_\mathbf{x}'(\mathbf{x},t):=\frac{\partial}{\partial\mathbf{x}}\mathbf{d}(\mathbf{x},t)$ and $\mathbf{b}_\mathbf{x}'(\mathbf{x},t):=\frac{\partial}{\partial\mathbf{x}}\mathbf{b}(\mathbf{x},t)$ exist. The unknown solution is: $\mathbf{x}=\mathbf{x}(t)\in\mathcal{D}\subset\mathbb{R}^m$, $t\in\mathcal{I}\subset\mathbb{R}$.

Now recall, a projector $\mathbf{Q}:\mathbb{R}^m\to\mathbb{R}^m$ is an operator such that $\mathbf{Q}^2=\mathbf{Q}$. For our later investigations we deal with a smaller class of DAEs with a so-called properly stated leading term.

Definition 3.1. (See [15].) The DAE (14) has a properly stated leading term if

$$\operatorname{Ker}\mathbf{A}\oplus\operatorname{Im}\mathbf{d}_\mathbf{x}'(\mathbf{x},t)=\mathbb{R}^n\quad\text{for all }\mathbf{x}\in\mathcal{D},\ t\in\mathcal{I},$$

and if there is a representing projector $\mathbf{R}\in C^1(\mathcal{I},\ \mathbb{R}^n)$, which satisfies: $\operatorname{Ker}\mathbf{A}=\operatorname{Ker}\mathbf{R}(t)$, $\operatorname{Im}\mathbf{d}_\mathbf{x}'(\mathbf{x},t)=\operatorname{Im}\mathbf{R}(t)$ and $\mathbf{d}(\mathbf{x},t)=\mathbf{R}(t)\mathbf{d}(\mathbf{x},t)$ for all $\mathbf{x}\in\mathcal{D}$ and $t\in\mathcal{I}$.

For the index definition, we need

Definition 3.2 *(Matrix chain and subspaces).* Given the DAE (14), we define recursively the following objects:

$$\mathbf{G}_0(\mathbf{x},t):=\mathbf{A}\mathbf{d}_\mathbf{x}'(\mathbf{x},t),$$

$$\mathbf{N}_0(\mathbf{x},t):=\operatorname{Ker}\mathbf{G}_0(\mathbf{x},t),$$

$$\mathbf{P}_0(\mathbf{x},t):=\mathbf{I}-\mathbf{Q}_0(\mathbf{x},t),\quad\mathbf{Q}_0(\mathbf{x},t)\text{ projector onto }\mathbf{N}_0(\mathbf{x},t),$$

$$\mathbf{S}_0(\mathbf{x},t):=\big\{\mathbf{z}\in\mathbb{R}^m\mid\mathbf{b}_\mathbf{x}'(\mathbf{x},t)\mathbf{z}\in\operatorname{Im}\mathbf{G}_0(\mathbf{x},t)\big\},$$

$$\mathbf{G}_1(\mathbf{x},t):=\mathbf{G}_0(\mathbf{x},t)+\mathbf{b}_\mathbf{x}'(\mathbf{x},t)\mathbf{Q}_0(\mathbf{x},t),$$

$$\mathbf{N}_1(\mathbf{x},t):=\operatorname{Ker}\mathbf{G}_1(\mathbf{x},t),$$

$$\mathbf{S}_1(\mathbf{x},t):=\big\{\mathbf{z}\in\mathbb{R}^m\mid\mathbf{b}_\mathbf{x}'(\mathbf{x},t)\mathbf{P}_0(\mathbf{x},t)\mathbf{z}\in\operatorname{Im}\mathbf{G}_1(\mathbf{x},t)\big\}.$$

Definition 3.3. (See [15].) The DAE (14) with a properly stated leading term is called DAE of (tractability) index-0 if

$$\mathbf{N}_0(\mathbf{x},t)=\{0\}\quad\text{for all }\mathbf{x}\in\mathcal{D},\ t\in\mathcal{I}$$

or otherwise it is called of index-1 if

$$(\mathbf{N}_0 \cap \mathbf{S}_0)(\mathbf{x}, t) = \{0\} \quad \text{for all } \mathbf{x} \in \mathcal{D}, \ t \in \mathcal{I}$$

or it is called of index-2 if

$$(\mathbf{N}_0 \cap \mathbf{S}_0)(\mathbf{x}, t) = \text{constant} \quad \text{and} \quad (\mathbf{N}_1 \cap \mathbf{S}_1)(\mathbf{x}, t) = \{0\} \quad \text{for all } \mathbf{x} \in \mathcal{D}, \ t \in \mathcal{I}.$$

Solving a DAE with a properly stated leading term is advantageous especially in index-1 and index-2 cases:

Remark 3.4. Often DAEs are not given with a properly stated leading term, and not all DAEs can be formulated as such. If possible, it is worth to formulate the properly stated leading term, because

- the leading term $\mathbf{d}(\mathbf{x}, t)$ figures out precisely which derivatives are actually involved and
- for a large class of index-1 and index-2 DAEs it can be shown that BDF and Runge–Kutta methods are stability preserving methods [12,13].

For electric circuits we refer to some standard results:

Remark 3.5. DAEs arising from MNA (and nodal analysis) with merely basic elements can always be formulated with a properly stated leading term [16] and the index does not exceed two, under the strictly passivity assumption [7]. More precisely, the MNA equations are of index-2 if and only if there are LI-cutsets (cutsets consisting of inductances and current sources only) or CV-loops (loops consisting of capacitances and voltage sources only) with at least one voltage source.

Rewriting the coupled problem (13) in the abstract form of (14) with properly stated leading term gives

$$\begin{bmatrix} \mathbf{A}_C & 0 & 0 \\ 0 & \mathbf{I} & 0 \\ 0 & 0 & 0 \\ 0 & 0 & \mathbf{M} \end{bmatrix} \frac{\mathrm{d}}{\mathrm{d}t} \begin{bmatrix} \mathbf{A}_C^+ \mathbf{A}_C \mathbf{q}_C(\cdot) \\ \boldsymbol{\Phi}_L(\cdot) \\ \mathbf{M}^+ \mathbf{M}\widehat{\mathbf{a}} \end{bmatrix} + \begin{bmatrix} \mathbf{A}_R \mathbf{g}_R(\cdot) + \mathbf{A}_L \mathbf{j}_L + \mathbf{A}_V \mathbf{j}_V + \mathbf{A}_M \mathbf{X}^\top \mathbf{K}(\cdot)\widehat{\mathbf{a}} + \mathbf{A}_I \mathbf{i}_s(t) \\ -\mathbf{A}_L^\top \mathbf{e} \\ \mathbf{A}_V^\top \mathbf{e} - \mathbf{v}_s(t) \\ \mathbf{K}(\cdot)\widehat{\mathbf{a}} - \mathbf{M}\mathbf{X}\mathbf{A}_M^\top \mathbf{e} \end{bmatrix} = 0 \tag{15}$$

and unknown $\mathbf{x} := [\mathbf{e}, \mathbf{j}_L, \mathbf{j}_V, \widehat{\mathbf{a}}]$.

Now, let $\mathbf{Q}_M$ be a constant projector onto $\operatorname{Ker}\mathbf{M}$, such that $\mathbf{Q}_M = \mathbf{Q}_M^\top$. Then for $\mathbf{P}_M = \mathbf{I} - \mathbf{Q}_M$ holds $\mathbf{P}_M = \mathbf{M}^+\mathbf{M}$, where '+' indicates the (Moore–Penrose) pseudo-inverse [8]. In fact, the DAE (15) has a properly stated leading term with representing projector

$$\mathbf{R} := \begin{bmatrix} \mathbf{A}_C^+ \mathbf{A}_C & 0 & 0 \\ 0 & \mathbf{I} & 0 \\ 0 & 0 & \mathbf{M}^+\mathbf{M} \end{bmatrix}.$$

Remark 3.6 (*Regularity*). From Assumption 2.6 follows

$$\operatorname{Ker}\bigl(\mathbf{M} + \mathbf{Q}_M^\top \mathbf{k}_a'(\cdot)\mathbf{Q}_M\bigr) = \{0\}.$$

The following property is clear from the construction of the distribution matrix and for other constructions it can easily be enforced:

Assumption 3.7 (*Soundness of excitation*). The distribution matrix $\mathbf{X}$ applies excitations only in conductive domains, i.e.,

$$\mathbf{X} = \mathbf{P}_M \mathbf{X}.$$

3.2. Index investigation

For an index-0 result we need to inspect

$$\mathbf{G}_0(\mathbf{x}, t) = \mathbf{A}\mathbf{d}_\mathbf{x}'(\mathbf{x}, t) = \begin{bmatrix} \mathbf{A}_C \mathbf{C}(\cdot)\mathbf{A}_C^\top & 0 & 0 & 0 \\ 0 & \mathbf{L}(\cdot) & 0 & 0 \\ 0 & 0 & 0 & 0 \\ 0 & 0 & 0 & \mathbf{M} \end{bmatrix}.$$

Theorem 3.8 (*Index-0*). *Let Assumptions* 2.3, 2.4 *and* 2.6 *be fulfilled. Then the DAE* (15) *has index-*0 *if and only if there is a tree containing capacitors only but no MQS device and no voltage source.*

Proof. We have to check that $\mathbf{G}_0(\mathbf{x}, t)$ is nonsingular. Noticing its block structure:

$$\mathbf{G}_0(\mathbf{x}, t) = \begin{bmatrix} \mathbf{E}(\cdot) & 0 \\ 0 & \mathbf{M} \end{bmatrix}$$

with the classical electric network components $\mathbf{E}$ (first three columns and rows), we realize that regularity of $\mathbf{G}_0$ is composed by (i) the usual regularity of $\mathbf{E}$ and (ii) regularity of $\mathbf{M}$.

(i) Standard case [7]. The proof is given for completeness: Since $\mathbf{C}$ and $\mathbf{L}$ are positive definite the matrix $\mathbf{G}_0$ is nonsingular if and only if the zero rows and columns disappear and $\operatorname{Ker} \mathbf{A}_C^\top = \{0\}$. The null space of $\operatorname{Ker} \mathbf{A}_C^\top$ is trivial if and only if the circuit has a tree containing capacitors only, see Remark 2.2. The block zero row and column disappear if and only if there is no voltage source in the circuit.
(ii) Lastly, $\operatorname{Ker} \mathbf{M} = \{0\}$ if and only if there is no MQS device. □

Remark 3.9.

(i) Obviously, if there is no MQS device, than we have the classical network case. Moreover, if there is an MQS device, then $\operatorname{Ker} \mathbf{M} \neq \{0\}$, i.e., the index is larger than zero.
(ii) Certainly, Theorem 3.8 can be extended to include MQS devices that consist of conducting materials only, i.e., $\operatorname{Ker} \mathbf{M} = \{0\}$. This particular case will not be discussed further on.

For the next step we need

$$\mathbf{Q}_0 = \begin{bmatrix} \mathbf{Q}_C & 0 & 0 & 0 \\ 0 & 0 & 0 & 0 \\ 0 & 0 & \mathbf{I} & 0 \\ 0 & 0 & 0 & \mathbf{Q}_M \end{bmatrix}, \qquad \mathbf{b}'_x(\mathbf{x}, t) = \begin{bmatrix} \mathbf{A}_R \mathbf{G}(\cdot) \mathbf{A}_R^\top & \mathbf{A}_L & \mathbf{A}_V & \mathbf{A}_M \mathbf{X}^\top \mathbf{k}'_a(\cdot) \\ -\mathbf{A}_L^\top & 0 & 0 & 0 \\ \mathbf{A}_V^\top & 0 & 0 & 0 \\ -\mathbf{M}\mathbf{X}\mathbf{A}_M^\top & 0 & 0 & \mathbf{k}'_a(\cdot) \end{bmatrix},$$

and

$$\mathbf{b}'_x(\mathbf{x}, t)\mathbf{Q}_0 = \begin{bmatrix} \mathbf{A}_R \mathbf{G}(\cdot) \mathbf{A}_R^\top \mathbf{Q}_C & 0 & \mathbf{A}_V & \mathbf{A}_M \mathbf{X}^\top \mathbf{k}'_a(\cdot) \mathbf{Q}_M \\ -\mathbf{A}_L^\top \mathbf{Q}_C & 0 & 0 & 0 \\ \mathbf{A}_V^\top \mathbf{Q}_C & 0 & 0 & 0 \\ -\mathbf{M}\mathbf{X}\mathbf{A}_M^\top \mathbf{Q}_C & 0 & 0 & \mathbf{k}'_a(\cdot) \mathbf{Q}_M \end{bmatrix},$$

where $\mathbf{Q}_0$, $\mathbf{Q}_C$ and $\mathbf{Q}_M$ are constant projectors onto $\operatorname{Ker} \mathbf{G}_0(\mathbf{x}, t)$, $\operatorname{Ker} \mathbf{A}_C^\top$ and $\operatorname{Ker} \mathbf{M}$, respectively. Consequently, also $\mathbf{Q}_0$ and $\mathbf{b}'_x(\mathbf{x}, t)$ are composed of a "classical" 3×3 block in the sense of [7] and a fourth block row/column that result from the coupling to the MQS device. The index-1 proof is a straightforward extension of [7].

Theorem 3.10 *(Index-1). Assumptions 2.3, 2.4 and 2.6 hold true and there is an MQS device, a voltage source or no tree containing capacitors only. The DAE (15) has index-1 if and only if there is neither an LIM-cutset (cutsets consisting of inductances, current sources and MQS devices only) nor a CV-loop with at least one voltage source.*

Proof. We need to compute $(\mathbf{N}_0 \cap \mathbf{S}_0)(\mathbf{x}, t)$. Let $\mathbf{W}_0(\mathbf{x}, t)$ be a projector along $\operatorname{Im} \mathbf{G}_0(\mathbf{x}, t)$; hence $\mathbf{W}_0^\top(\mathbf{x}, t)$ is a projector onto $\operatorname{Ker} \mathbf{G}_0^\top(\mathbf{x}, t)$. Since $\operatorname{Ker} \mathbf{G}_0^\top(\mathbf{x}, t) = \operatorname{Ker} \mathbf{G}_0(\mathbf{x}, t)$ holds, we can choose $\mathbf{W}_0^\top(\mathbf{x}, t) = \mathbf{Q}_0$. For $\mathbf{S}_0$ we find:

$$\mathbf{S}_0(\mathbf{x}, t) = \left\{ \mathbf{z} \in \mathbb{R}^m \mid \mathbf{b}'_x(\mathbf{x}, t)\mathbf{z} \in \operatorname{Im} \mathbf{G}_0(\mathbf{x}, t) \right\} = \left\{ \mathbf{z} \in \mathbb{R}^m \mid \mathbf{W}_0(\mathbf{x}, t)\mathbf{b}'_x(\mathbf{x}, t)\mathbf{z} = 0 \right\} = \left(\mathbf{W}_0 \mathbf{b}'_x \right)(\mathbf{x}, t).$$

This gives using also the projector $\mathbf{Q}_0$

$$(\mathbf{N}_0 \cap \mathbf{S}_0)(\mathbf{x}, t) = \operatorname{Ker} \mathbf{G}_0(\mathbf{x}, t) \cap \operatorname{Ker}\left(\mathbf{W}_0 \mathbf{b}'_x\right)(\mathbf{x}, t) = \operatorname{Im} \mathbf{Q}_0 \cap \operatorname{Ker} \mathbf{W}_0 \mathbf{b}'_x(\mathbf{x}, t)\mathbf{Q}_0.$$

Let $\mathbf{z} = [\mathbf{z}_1 \ \mathbf{z}_2 \ \mathbf{z}_3 \ \mathbf{z}_4]^\top \in (\mathbf{N}_0 \cap \mathbf{S}_0)(\mathbf{x}, t)$. Then (a) $\mathbf{Q}_0 \mathbf{z} = \mathbf{z}$ and (b) $\mathbf{W}_0 \mathbf{b}'_x(\mathbf{x}, t)\mathbf{Q}_0 \mathbf{z} = 0$. We first treat the magnetic part $\mathbf{z}_4$: For (a), the block diagonal structure of $\mathbf{Q}_0$ gives $\mathbf{z}_4 = \mathbf{Q}_M \mathbf{z}_4$. For (b), we inspect

$$\mathbf{W}_0 \mathbf{b}'_x(\mathbf{x}, t)\mathbf{Q}_0 = \begin{bmatrix} \mathbf{Q}_C^\top \mathbf{A}_R \mathbf{G}(\cdot) \mathbf{A}_R^\top \mathbf{Q}_C & 0 & \mathbf{Q}_C^\top \mathbf{A}_V & \mathbf{Q}_C^\top \mathbf{A}_M \mathbf{X}^\top \mathbf{k}'_a(\cdot) \mathbf{Q}_M \\ 0 & 0 & 0 & 0 \\ \mathbf{A}_V^\top \mathbf{Q}_C & 0 & 0 & 0 \\ 0 & 0 & 0 & \mathbf{Q}_M^\top \mathbf{k}'_a(\cdot) \mathbf{Q}_M \end{bmatrix}, \qquad (16)$$

and find $\mathbf{Q}_M \mathbf{z}_4 = 0$, since $\mathbf{Q}_M^\top \mathbf{M} = 0$ and the last block row of (16) gives

$$\mathbf{Q}_M^\top\big(\mathbf{M} + \mathbf{k}_a'(\cdot)\big)\mathbf{Q}_M\mathbf{z}_4 = 0,$$

with $\mathbf{M} + \mathbf{k}_a'(\cdot)$ positive definite by Assumption 2.6. Hence (a) and (b) imply

$$\mathbf{z}_4 = 0. \tag{17}$$

Thus we have

$$(\mathbf{N}_0 \cap \mathbf{S}_0)(\mathbf{x}, t) = \big(\mathrm{Im}(\mathbf{Q}_0)^E \cap \mathrm{Ker}\big(\mathbf{W}_0\mathbf{b}_x'(\mathbf{x}, t)\mathbf{Q}_0\big)^E\big) \times \{0\},$$

where superscript E denoting the standard circuit block (first three rows and first three columns). Now, from standard circuit results [7], we know

$$\mathbf{z}_1 \in \mathrm{Ker}[\mathbf{A}_C\ \mathbf{A}_R\ \mathbf{A}_V]^\top, \qquad \mathbf{z}_2 = 0, \quad \text{and} \quad \mathbf{Q}_C^\top\mathbf{A}_V\mathbf{z}_3 = 0. \tag{18}$$

Finally from (17)–(18) we obtain: $(\mathbf{N}_0 \cap \mathbf{S}_0)(\mathbf{x}, t) = \{0\}$ holds if and only if there is neither an *LIM*-cutset (Remark 2.2) nor a *CV*-loop (Remark 2.2) with at least one voltage source. $\square$

Remark 3.11. For completeness, we give the standard reasoning for the circuit contribution (18): Using $\mathbf{z}_4 = 0$, $\mathbf{z} \in \mathrm{Im}\,\mathbf{Q}_0$ implies

$$\mathbf{Q}_C\mathbf{z}_1 = \mathbf{z}_1, \qquad \mathbf{z}_2 = 0, \tag{19}$$

and $\mathbf{z} \in \mathrm{Ker}\,\mathbf{W}_0\mathbf{b}_x'(\mathbf{x}, t)\mathbf{Q}_0$ implies

$$\mathbf{Q}_C^\top\mathbf{A}_R\mathbf{G}(\cdot)\mathbf{A}_R^\top\mathbf{Q}_C\mathbf{z}_1 + \mathbf{Q}_C^\top\mathbf{A}_V\mathbf{z}_3 = 0, \tag{20}$$
$$\mathbf{A}_V^\top\mathbf{Q}_C\mathbf{z}_1 = 0. \tag{21}$$

Left-multiplying (20) by $\mathbf{z}_1^\top$ and using (21), we conclude that $\mathbf{z}_1 \in \mathrm{Ker}\,\mathbf{A}_R^\top\mathbf{Q}_C$ and thus $\mathbf{Q}_C^\top\mathbf{A}_V\mathbf{z}_3 = 0$. Now, using (19), we find indeed (18).

We introduce the constant projector $\mathbf{Q}_{CRV}$ onto $\mathrm{Ker}[\mathbf{A}_C\ \mathbf{A}_R\ \mathbf{A}_V]^\top$ with $\mathbf{Q}_{CRV} = \mathbf{Q}_C\mathbf{Q}_{V-C}\mathbf{Q}_{R-CV}$ where $\mathbf{Q}_{C-V}$, $\mathbf{Q}_{V-C}$ and $\mathbf{Q}_{R-CV}$ are constant projectors onto $\mathrm{Ker}\,\mathbf{Q}_C^\top\mathbf{A}_V$, $\mathrm{Ker}\,\mathbf{A}_V^\top\mathbf{Q}_C$ and $\mathrm{Ker}\,\mathbf{A}_R^\top\mathbf{Q}_C\mathbf{Q}_{V-C}$, respectively, see [7]. With these new projectors we directly obtain:

Lemma 3.12. *The intersection* $(\mathbf{N}_0 \cap \mathbf{S}_0)(\mathbf{x}, t)$ *can be described by*

$$(\mathbf{N}_0 \cap \mathbf{S}_0)(\mathbf{x}, t) = \big\{z \in \mathbb{R}^n \ \big|\ \mathbf{z}_1 \in \mathrm{Im}\,\mathbf{Q}_{CRV},\ \mathbf{z}_3 \in \mathrm{Im}\,\mathbf{Q}_{C-V},\ [\mathbf{z}_2\ \mathbf{z}_4] = 0\big\}.$$

Thus, the dimension of $(\mathbf{N}_0 \cap \mathbf{S}_0)(\mathbf{x}, t)$ *is constant.*

Notice, the constant dimension is important for the index-2 case.

Remark 3.13. Let $\mathbf{Q}$, $\mathbf{B}$ and $\mathbf{B}^+$ denote a projector, a matrix and its (Moore–Penrose) pseudo-inverse, respectively. If $\mathbf{B} = \mathbf{Q}^\top\mathbf{B}\mathbf{Q}$ then it follows $\mathbf{B}^+ = \mathbf{Q}\mathbf{B}^+\mathbf{Q}^\top$.

Lemma 3.14 *(Consistent excitation). Let Assumptions* 2.6 *and* 3.7 *be fulfilled, then*

$$\mathbf{X}^\top\mathbf{H}_\mathbf{k}(\cdot)\mathbf{X} \quad \text{with } \mathbf{H}_\mathbf{k}(\cdot) := \mathbf{k}_a'(\cdot)\big(\mathbf{k}_a'(\cdot)^+ - \big(\mathbf{Q}_M^\top\mathbf{k}_a'(\cdot)\mathbf{Q}_M\big)^+\big)\mathbf{k}_a'(\cdot)$$

is positive definite.

Proof. A straightforward computation using the soundness of the excitation (Assumption 3.7), properties of the projector and pseudo-inverse (Remark 3.13) and the divergence-freeness of the excitation (9), i.e., $\tilde{\mathbf{S}}\mathbf{M}\mathbf{X} = 0$ yields

$$\mathbf{X}^\top\mathbf{H}_\mathbf{k}(\cdot)\mathbf{X} = \mathbf{X}^\top\mathbf{T}\mathbf{Z}_\mathbf{k}(\cdot)\mathbf{T}^\top\mathbf{X}$$

with a fully regularized curl–curl matrix $\mathbf{Z}_\mathbf{k}(\cdot) := \mathbf{k}_a'(\cdot) + \mathbf{M}^\top\tilde{\mathbf{S}}^\top\tilde{\mathbf{S}}\mathbf{M}$ and the block-elimination $\mathbf{T}(\cdot) := \mathbf{I} - (\mathbf{P}_M^\top\mathbf{Z}_\mathbf{k}(\cdot)\mathbf{Q}_M) \cdot (\mathbf{Q}_M^\top\mathbf{Z}_\mathbf{k}(\cdot)\mathbf{Q}_M)^+$.

The matrix $\mathbf{T}(\cdot)$ is regular with $\mathbf{T}^{-1}(\cdot) = \mathbf{I} + (\mathbf{P}_M^\top\mathbf{Z}_\mathbf{k}(\cdot)\mathbf{Q}_M)(\mathbf{Q}_M^\top\mathbf{Z}_\mathbf{k}(\cdot)\mathbf{Q}_M)^+$ and $\mathbf{X}$ has full column rank by construction. Thus the positive definiteness of $\mathbf{Z}_\mathbf{k}(\cdot)$ must be shown, where the only interesting elements are from $\ker\mathbf{C} = \mathrm{im}\,\tilde{\mathbf{S}}^\top$ due to the structure of $\mathbf{k}_a'$ (7). This gives:

$$\mathbf{x}^\top\tilde{\mathbf{S}}\big(\mathbf{Y} + \mathbf{M}^\top\tilde{\mathbf{S}}^\top\tilde{\mathbf{S}}\mathbf{M}\big)\tilde{\mathbf{S}}^\top\mathbf{x} > 0 \quad \text{for all } \mathbf{x} \neq 0$$

with $\mathbf{Y}$ as defined in Assumption 2.6. Positive definiteness follows in both cases

1. if $\tilde{\mathbf{S}}^\top \mathbf{x} \in \ker \mathbf{M}$ then there is a $\mathbf{y}$ such that $\tilde{\mathbf{S}}^\top \mathbf{x} = \mathbf{Q}_M \mathbf{y}$. Thus the second summand vanishes and the first summand is positive because of Assumption 2.6;
2. else $\mathbf{M}\tilde{\mathbf{S}}^\top \mathbf{x} \neq 0$ and thus the second summand is positive (because its kernel is $\ker \mathbf{M}\tilde{\mathbf{S}}^\top$) and the first summand is non-negative. □

Remark 3.15. In 2D the curl–curl operator equals the Laplacian [11]. Therefore the corresponding curl–curl matrix is positive definite and thus (3.14) holds for 2D models without Assumption 2.6 (i.e., without gauging).

Next, for index-2 we compute $\mathbf{G}_1(\mathbf{x}, t) = \mathbf{G}_0(\mathbf{x}, t) + \mathbf{b}'_x(\mathbf{x}, t)\mathbf{Q}_0$ from the matrix chain:

$$\mathbf{G}_1(\mathbf{x}, t) = \begin{bmatrix} \mathbf{A}_C \mathbf{C}(\cdot)\mathbf{A}_C^\top + \mathbf{A}_R \mathbf{G}(\cdot)\mathbf{A}_R^\top \mathbf{Q}_C & 0 & \mathbf{A}_V & \mathbf{A}_M \mathbf{X}^\top \mathbf{k}'_a(\cdot)\mathbf{Q}_M \\ -\mathbf{A}_L^\top \mathbf{Q}_C & \mathbf{L}(\cdot) & 0 & 0 \\ \mathbf{A}_V^\top \mathbf{Q}_C & 0 & 0 & 0 \\ -\mathbf{M}\mathbf{X}\mathbf{A}_M^\top \mathbf{Q}_C & 0 & 0 & \mathbf{M} + \mathbf{k}'_a(\cdot)\mathbf{Q}_M \end{bmatrix}.$$

In contrast to [7], we will not calculate a projector $\mathbf{Q}_1$ onto $\ker \mathbf{G}_1(\mathbf{x}, t)$ to prove the following theorem.

Theorem 3.16 (Index-2). *Let Assumptions 2.3, 2.4, 2.6 and 3.7 hold true and there is at least one MQS device, voltage source or no tree containing capacitors only. Then the DAE* (15) *has index-2 if and only if there is an LIM-cutset or a CV-loop with at least one voltage source.*

Proof. We show that $(\mathbf{N}_1 \cap \mathbf{S}_1)(\mathbf{x}, t)$ is trivial. We choose $\mathbf{W}_1(\mathbf{x}, t)$ as

$$\mathbf{W}_1(\mathbf{x}, t) = \begin{bmatrix} \mathbf{Q}_{CRV}^\top & 0 & 0 & -\mathbf{Q}_{CRV}^\top \mathbf{A}_M \mathbf{X}^\top \mathbf{k}'_a(\cdot)(\mathbf{Q}_M^\top \mathbf{k}'_a(\cdot)\mathbf{Q}_M)^+ \\ 0 & 0 & 0 & 0 \\ 0 & 0 & \mathbf{Q}_{C-V}^\top & 0 \\ 0 & 0 & 0 & 0 \end{bmatrix}$$

where $(\mathbf{Q}_M^\top \mathbf{k}'_a(\cdot)\mathbf{Q}_M)^+ = \mathbf{Q}_M(\mathbf{Q}_M^\top \mathbf{k}'_a(\cdot)\mathbf{Q}_M)^+ \mathbf{Q}_M^\top$ (see Remark 3.13) and $\mathbf{W}_1(\mathbf{x}, t)$ is a projector with $\operatorname{Im}\mathbf{G}_1(\mathbf{x}, t) \subset \ker \mathbf{W}_1(\mathbf{x}, t)$. We have

$$\mathbf{S}_1(\mathbf{x}, t) = \left\{ z \in \mathbb{R}^n \,\middle|\, \mathbf{b}'_x(\mathbf{x}, t)\mathbf{P}_0 z \in \operatorname{Im}\mathbf{G}_1(\mathbf{x}, t) \right\}$$
$$\subset \left\{ z \in \mathbb{R}^n \,\middle|\, \mathbf{W}_1(\mathbf{x}, t)\mathbf{b}'_x(\mathbf{x}, t)\mathbf{P}_0 z = 0 \right\} =: \widetilde{\mathbf{S}}_1(\mathbf{x}, t)$$

and we will show that even $(\mathbf{N}_1 \cap \widetilde{\mathbf{S}}_1)(\mathbf{x}, t)$ is trivial; since $\mathbf{S}_1(\mathbf{x}, t) \subset \widetilde{\mathbf{S}}_1(\mathbf{x}, t)$ holds, we obtain the desired result. To this end, we compute

$$\mathbf{W}_1(\mathbf{x}, t)\mathbf{b}'_x(\mathbf{x}, t)\mathbf{P}_0 = \begin{bmatrix} 0 & \mathbf{Q}_{CRV}^\top \mathbf{A}_L & 0 & \mathbf{Q}_{CRV}^\top \mathbf{A}_M \mathbf{X}^\top \mathbf{H_k}(\cdot)\mathbf{P}_M \\ 0 & 0 & 0 & 0 \\ \mathbf{Q}_{C-V}^\top \mathbf{A}_V^\top \mathbf{P}_C & 0 & 0 & 0 \\ 0 & 0 & 0 & 0 \end{bmatrix},$$

with $\mathbf{H_k}(\cdot) = \mathbf{k}'_a(\cdot)(\mathbf{k}'_a(\cdot)^+ - (\mathbf{Q}_M^\top \mathbf{k}'_a(\cdot)\mathbf{Q}_M)^+)\mathbf{k}'_a(\cdot)$. Now, from the equation $(\mathbf{W}_1 \mathbf{b}'_x)(\mathbf{x}, t)\mathbf{P}_0 z = 0$ follows

$$\mathbf{Q}_{CRV}^\top \mathbf{A}_L \mathbf{z}_2 + \mathbf{Q}_{CRV}^\top \mathbf{A}_M \mathbf{X}^\top \mathbf{H_k}(\cdot)\mathbf{P}_M \mathbf{z}_4 = 0, \tag{22}$$
$$\mathbf{Q}_{C-V}^\top \mathbf{A}_V^\top \mathbf{P}_C \mathbf{z}_1 = 0, \tag{23}$$

and $\mathbf{G}_1(\mathbf{x}, t)z = 0$ gives

$$\left(\mathbf{A}_C \mathbf{C}(\cdot)\mathbf{A}_C^\top + \mathbf{A}_R \mathbf{G}(\cdot)\mathbf{A}_R^\top \mathbf{Q}_C\right)\mathbf{z}_1 + \mathbf{A}_V \mathbf{z}_3 + \mathbf{A}_M \mathbf{X}^\top \mathbf{k}'_a(\cdot)\mathbf{Q}_M \mathbf{z}_4 = 0, \tag{24}$$
$$\mathbf{z}_2 - \mathbf{L}^{-1}(\cdot)\mathbf{A}_L^\top \mathbf{Q}_C \mathbf{z}_1 = 0, \tag{25}$$
$$\mathbf{A}_V^\top \mathbf{Q}_C \mathbf{z}_1 = 0, \tag{26}$$
$$-\mathbf{M}\mathbf{X}\mathbf{A}_M^\top \mathbf{Q}_C \mathbf{z}_1 + \left(\mathbf{M} + \mathbf{k}'_a(\cdot)\mathbf{Q}_M\right)\mathbf{z}_4 = 0. \tag{27}$$

Left-multiplying (27) by $(\mathbf{Q}_M \mathbf{z}_4)^\top$, we obtain

$$\mathbf{Q}_M \mathbf{z}_4 = 0, \quad \text{that is,} \quad \mathbf{z}_4 = \mathbf{P}_M \mathbf{z}_4, \tag{28}$$

because $\mathbf{M} + \mathbf{k}'_a(\cdot)$ is positive definite by Assumption 2.6.

From (27) with $\mathbf{P}_M = \mathbf{M}^+ \mathbf{M}$ and $\mathbf{z}_4 = \mathbf{P}_M \mathbf{z}_4$, we can conclude that

$$\mathbf{z}_4 = \mathbf{X}\mathbf{A}_M^\top \mathbf{Q}_C \mathbf{z}_1, \tag{29}$$

since it holds $\mathbf{X} = \mathbf{P}_M \mathbf{X}$ using Assumption 3.7. Multiplying (24) from left by $(\mathbf{Q}_C \mathbf{z}_1)^\top$, using both (26) and (28), we obtain

$$\mathbf{Q}_C \mathbf{z}_1 \in \text{Ker}\, \mathbf{A}_R^\top. \tag{30}$$

Putting (25), (30) and the definition of $\mathbf{Q}_C$ together, we have

$$\mathbf{Q}_C \mathbf{z}_1 \in \text{Ker}[\mathbf{A}_C\, \mathbf{A}_R\, \mathbf{A}_V]^\top = \text{Im}\, \mathbf{Q}_{CRV}$$

that is, $\mathbf{Q}_C \mathbf{z}_1 = \mathbf{Q}_{CRV} \mathbf{Q}_C \mathbf{z}_1$. Inserting (25) and (29) into (22) gives

$$\mathbf{Q}_{CRV}^\top \mathbf{A}_L \mathbf{L}^{-1}(\cdot)\mathbf{A}_L^\top \mathbf{Q}_C \mathbf{z}_1 + \mathbf{Q}_{CRV}^\top \mathbf{A}_M \mathbf{X}^\top \mathbf{H_k}(\cdot)\mathbf{X}\mathbf{A}_M^\top \mathbf{Q}_C \mathbf{z}_1 = 0$$

where $\mathbf{X}^\top \mathbf{H_k}(\cdot)\mathbf{X}$ is positive definite due to (3.14). Therefore it follows that $\mathbf{A}_L^\top \mathbf{Q}_C \mathbf{z}_1 = 0$ and $\mathbf{A}_M^\top \mathbf{Q}_C \mathbf{z}_1 = 0$ (using $\mathbf{Q}_C \mathbf{z}_1 = \mathbf{Q}_{CRV} \mathbf{Q}_C \mathbf{z}_1$). Hence $\mathbf{Q}_C \mathbf{z}_1 \in \text{Ker}[\mathbf{A}_C\, \mathbf{A}_R\, \mathbf{A}_L\, \mathbf{A}_V\, \mathbf{A}_M]^\top$, which is trivial due to Assumption 2.4.

Thus we find $\mathbf{Q}_C \mathbf{z}_1 = 0$, in other words, $\mathbf{P}_C \mathbf{z}_1 = \mathbf{z}_1$. From (25) we deduce $\mathbf{z}_2 = 0$. Using this, (24) can be written as

$$\mathbf{H_C}(\cdot)\mathbf{P}_C \mathbf{z}_1 = -\mathbf{A}_V \mathbf{z}_3,$$

where $\mathbf{H_C}(\cdot) = \mathbf{A}_C \mathbf{C}(\cdot)\mathbf{A}_C^\top + \mathbf{Q}_C^\top \mathbf{Q}_C$ is positive definite. Thus

$$\mathbf{z}_1 = -\mathbf{H_C}(\cdot)^{-1}\mathbf{A}_V \mathbf{z}_3.$$

Multiplying (24) from left by $\mathbf{Q}_C^\top$ leads to $\mathbf{Q}_C^\top \mathbf{A}_V \mathbf{z}_3 = 0$ and $\mathbf{z}_3 \in \text{Im}\, \mathbf{Q}_{C-V}$ respectively. Together with (23) and $\mathbf{z}_3 \in \text{Im}\, \mathbf{Q}_{C-V}$ this gives

$$\mathbf{Q}_{C-V}^\top \mathbf{A}_V^\top \mathbf{H_C}(\cdot)^{-1}\mathbf{A}_V \mathbf{Q}_{C-V} \mathbf{z}_3 = 0.$$

Hence we can conclude $\mathbf{A}_V \mathbf{z}_3 = 0$ and from this we have $\mathbf{z}_3 = 0$, since $\mathbf{A}_V$ has full column rank. Consequently from $\mathbf{H_C}(\cdot)\mathbf{z}_1 = 0$ follows $\mathbf{z}_1 = 0$. Hence $(\mathbf{N}_1 \cap \widetilde{\mathbf{S}}_1)(\mathbf{x}, t)$ and $(\mathbf{N}_1 \cap \mathbf{S}_1)(\mathbf{x}, t)$ are trivial if and only if there is an *LIM*-cutset or a *CV*-loop with at least one voltage source. $\quad\square$

Remark 3.17 *(Flux/charge MNA).* Notice flux/charge oriented MNA [7], or the introduction of $\mathbf{j}_M$ as an additional unknown of our coupled problem (cf. Section 2.3) do not change our index-1 and index-2 results.

Corollary 3.18 *(Linear index-2). The index-2 variables are those components that depend on first derivatives of the input functions. In our case they can be described by* $\mathbf{Tx}$ *[6], where* $\mathbf{T}$ *is a constant projector onto* $(\mathbf{N}_0 \cap \mathbf{S}_0)(\mathbf{x}, t)$ *with*

$$\mathbf{T} = \begin{bmatrix} \mathbf{Q}_{CRV} & 0 & 0 & 0 \\ 0 & 0 & 0 & 0 \\ 0 & 0 & \mathbf{Q}_{C-V} & 0 \\ 0 & 0 & 0 & 0 \end{bmatrix}.$$

Then we can write in the general DAE (14): $\mathbf{b}(\mathbf{x}, t) = \mathbf{b}(\mathbf{Ux}, t) + \mathbf{BTx}$ *for a problem given matrix* $\mathbf{B}$ *and* $\mathbf{d}(\mathbf{x}, t) = \mathbf{d}(\mathbf{Ux}, t)$ *with* $\mathbf{U} = \mathbf{I} - \mathbf{T}$. *Thus index-2 variables enter our system linearly.*

Using perturbation-index analysis, it has been shown for index-2 Hessenberg systems with linear index-2 variables [1], and for index-2 circuits [21], that the numerical difficulties in time-integration are moderate, because the differential (index-0) variables are not affected by numerical differentiations.

Remark 3.19 *(Consistent initialization).* To solve a DAE numerically, it is important to start with a consistent initial value because we cannot choose initial values arbitrarily as in case of an ordinary differential equation [10,6,16]. Consistent initial values are obtained by standard techniques that require in the index-1 case the solution of a system of nonlinear equations [16]. In the case of an index-2 DAE, the calculation of a consistent initialization becomes more complicated. At least for DAEs with linear index-2 components we can obtain a consistent value after one (implicit) Euler integration step starting from an operation point [6].

4. Numerical example

We will prove the numerical importance of the index results by discussing two simple examples that illustrate the different behavior of the index-1 and index-2 cases. The most simple problems are the following, see Fig. 2,

(a) a circuit with no devices but a voltage source and a one-port MQS device ($\mathbf{A}_V = [1]$ and $\mathbf{A}_M = [-1]$) states an index-1 problem (see Fig. 2(a)),
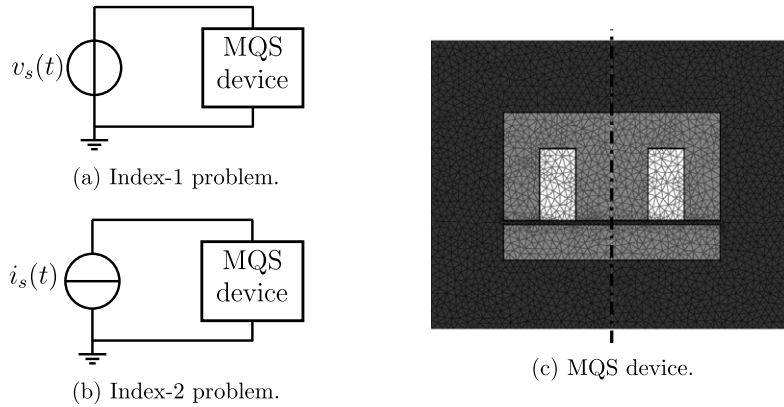
Fig. 2. Examples: (a) voltage-driven MQS device is index-1, (b) current-driven MQS device is index-2, (c) 2D 'EI'-inductor model discretized by FEMM [17]: rotational symmetric $(- \cdot -)$, coupled to the circuit via its coil (white), 'EI'-core (grey), air (black).

(b) a circuit with no devices but a current source and a one-port MQS device ($\mathbf{A}_\mathrm{I} = [1]$ and $\mathbf{A}_\mathrm{M} = [-1]$) states an index-2 problem (see Fig. 2(b)).

The tractability indices of those particular problems agree with the Kronecker index and differentiation index results in [19,23].

The simplest one-port MQS device is a (linear) inductor without eddy currents. Fig. 2(c) shows the 2D model of such a coil with an 'EI'-core.[1] It is spatially discretized by FEMM [17]. In this simple linear setup the PDE model is equivalent to a series connection of a lumped resistance R and an inductance L [14]. Hence, for this simple problem, we have the analytic solution of the voltages and currents of the coupled DAE problem at hand: in the index-2 setting, cf. Fig. 2(b), with a sinusoidal current source

$$i_\mathrm{s}(t) = \sin(2\pi f t), \quad \text{with a frequency } f = 50 \text{ Hz},$$

the voltage drop (at the RL-element) is analytically given by

$$v_\mathrm{M} = \mathbf{A}_\mathrm{M}^\top \mathbf{e} = \mathbf{A}_\mathrm{M}^\top \left(R i_\mathrm{s}(t) + L \frac{\mathrm{d}}{\mathrm{d}t} i_\mathrm{s}(t) \right) = -R \sin(2\pi f t) - 2\pi f L \cos(2\pi f t).$$

In the index-1 case, cf. Fig. 2(a), a voltage source is connected to the MQS device, i.e., $v_\mathrm{M}(t) = v_\mathrm{s}(t)$ and $i_\mathrm{L}(t) = i_\mathrm{s}(t)$.

The following simulations were carried out by the implicit Euler scheme applied to the respective coupled system and results are compared to the analytical reference solution given above. Higher-order time-integration methods could be applied analogously, but would not give further inside. Fig. 3 shows the numerical error due to time-integration for fixed time step sizes $h = 10^{-11}$ s, $\dots$, 10^{-6} s. Although both, the index-1 and index-2 circuits describe the same physical phenomenon, the error behaves differently: in the index-1 case, Fig. 3(a), the relative error decreases with the step size as one would expect. It oscillates for the smallest step size $h = 10^{-11}$s, where errors are near to machine precision. On the other hand, in the index-2 case Fig. 3(b), the numerical error is highly oscillating for step sizes below $h = 10^{-8}$s. Moreover, below $h = 10^{-8}$ the error increases for decreasing step size. Nonetheless those errors are not propagated in time because they do not affect the differential components, see Corollary 3.18. Only when using a step size control, one has to take special care, i.e., exclude the index-2 voltages from the set of variables that are monitored, such that the oscillations do not require unreasonable step sizes.

A similar error characteristics can be observed in simulations where the PDE model is substituted by a lumped inductance model. This underlines that the device is topologically equivalent to an inductance.

5. Conclusion

We have modeled a network of lumped resistors, inductors, capacitors, independent current and voltage sources, and spatially distributed MQS devices by applying MNA. Starting from spatially discretized MQS devices, we have deduced a coupled system of DAEs with properly stated leading term. Then the structural properties of this system have been analyzed: We have proven that the index does not exceed two under certain conditions. Thereby the proofs for index-0 and index-1 extend the known electric circuit technique by the treatment of MQS devices variables and equations. For the index-2 case, the consistency of the MQS device excitation is a crucial first step and our proof is not based on the explicit computation

---

[1] Details are given at http://www.femm.info/wiki/InductanceExample.

(a) relative error in current (index-1)   (b) relative error in voltage (index-2)
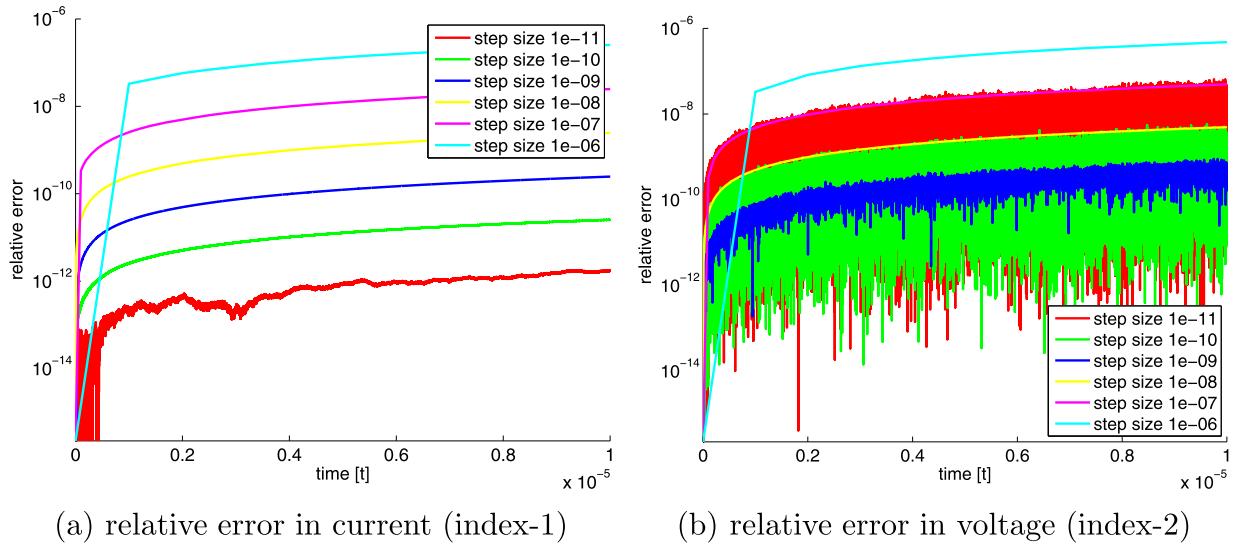
Fig. 3. Numerical errors for (a) the index-1 problem (voltage driven) and (b) the index-2 problem (current driven).

of the respective projector. Thus we have generalized the topological index criteria of electrical circuits. A simple numerical example illustrated the findings and demonstrated that the coupled simulation does not suffer from error propagation in the index-2 variables due to linear dependence of corresponding variables.

Although the MQS devices are modeled as controlled current sources, our structural analysis shows that they behave topologically as inductances. This corresponds to the physical effects covered by the eddy current problem.

Acknowledgements

References

[1] M. Arnold, K. Strehmel, R. Weiner, Errors in the numerical solution of nonlinear differential-algebraic systems of index 2, Technical Report, Martin Luther Universität Halle–Wittenberg, 1995.
[2] S. Baumanns, M. Selva Soto, C. Tischendorf, Consistent initialization for coupled circuit-device simulation, in: J. Roos, L.R. Costa (Eds.), Scientific Computing in Electrical Engineering, SCEE 2008, vol. 14, Springer, Berlin, 2010, pp. 297–304.
[3] M. Clemens, T. Weiland, Regularization of eddy-current formulations using discrete grad-div operators, IEEE Trans. Magn. 38 (2002) 569–572.
[4] H. De Gersem, T. Weiland, Field-circuit coupling for time-harmonic models discretized by the finite integration technique, IEEE Trans. Magn. 40 (2004) 1334–1337.
[5] G. Denk, Circuit simulation for nanoelectronics, in: H.G. Bock, F. Hoog, A. Friedman, A. Gupta, H. Neunzert, W.R. Pulleyblank, T. Rusten, F. Santosa, A.K. Tornberg, V. Capasso, R. Mattheij, H. Neunzert, O. Scherzer, A. Anile, G. Alì, G. Mascali (Eds.), Scientific Computing in Electrical Engineering, in: Mathematics in Industry, vol. 9, Springer, Berlin, Heidelberg, 2006, pp. 13–20.
[6] D. Estévez Schwarz, Consistent initialization for index-2 differential algebraic equations and its application to circuit simulation, PhD thesis, Humboldt Univ. zu Berlin, 2000.
[7] D. Estévez Schwarz, C. Tischendorf, Structural analysis of electric circuits and consequences for MNA, Int. J. Circ. Theor. Appl. 28 (2000) 131–162.
[8] G.H. Golub, C.F. van Loan, Matrix Computations, The Johns Hopkins University Press, 1996.
[9] E. Griepentrog, R. März, Differential-Algebraic Equations and Their Numerical Treatment, Teubner, Leipzig, 1986.
[10] E. Hairer, G. Wanner, Solving Ordinary Differential Equations II: Stiff and Differential-Algebraic Problems, Springer, Berlin, 1991.
[11] H.A. Haus, J.R. Melcher, Electromagnetic Fields and Energy, Prentice-Hall, 1989.
[12] I. Higueras, R. März, C. Tischendorf, Stability preserving integration of index-1 DAEs, Appl. Numer. Math. 45 (2003) 175–200.
[13] I. Higueras, R. März, C. Tischendorf, Stability preserving integration of index-2 DAEs, Appl. Numer. Math. 45 (2003) 201–229.
[14] D.A. Lowther, P.P. Silvester, Computer-Aided Design in Magnetics, Springer, Berlin, 1986.
[15] R. März, Nonlinear differential-algebraic equations with properly formulated leading term, Technical report 01-3, Humboldt Univ. zu Berlin, 2001.
[16] R. März, Differential algebraic systems with properly stated leading term and MNA equations, Technical Report 2002-13, Humboldt Univ. zu Berlin, 2002.
[17] D. Meeker, Finite element method magnetics user's manual. Version 4.2 (09Nov2010 Build), 2010.
[18] J. Roos, L.R. Costa (Eds.), Scientific Computing in Electrical Engineering, SCEE 2008, vol. 14, Springer, Berlin, 2010.

[19] S. Schöps, A. Bartel, H. De Gersem, M. Günther, DAE-index and convergence analysis of lumped electric circuits refined by 3-d MQS conductor models, in: J. Roos, L.R. Costa (Eds.), Scientific Computing in Electrical Engineering, SCEE 2008, vol. 14, Springer, Berlin, 2010, pp. 341–350.
[20] M. Selva Soto, C. Tischendorf, Numerical analysis of DAEs from coupled circuit and semiconductor simulation, Appl. Numer. Math. 53 (2005) 471–488.
[21] C. Tischendorf, Model design criteria for integrated circuits to have a unique solution and good numerical properties, in: U. van Rienen, M. Günther, D. Hecht (Eds.), Scientific Computing in Electrical Engineering, SCEE 2000, Springer, Berlin, 2001, pp. 179–198.
[22] C. Tischendorf, Coupled systems of differential algebraic and partial differential equations in circuit and device simulation. Modeling and numerical analysis. Habilitation thesis, Humboldt Univ. zu Berlin, 2004.
[23] I. Tsukerman, Finite element differential-algebraic systems for eddy current problems, Numer. Algorithms 31 (2002) 319–335.
[24] T. Weiland, A discretization model for the solution of Maxwell's equations for six-component fields, AEU 31 (1977) 116–120.